ISSN 0965-5425, Computational Mathematics and Mathematical Physics, 2019, Vol. 59, No. 9, pp. 1493–1507. © Pleiades Publishing, Ltd., 2019.
Russian Text © The Author(s), 2019, published in Zhurnal Vychislitel'noi Matematiki i Matematicheskoi Fiziki, 2019, Vol. 59, No. 9, pp. 1554–1569.

Mathematical Modeling of Tropical Cyclones on the Basis of Wind Trajectories

M. Aouaouda[a],*, A. Ayadi[a],, and H. Fujita Yashima[b],*****

[a] *Université d'Oum El Bouaghi, Oum, Algérie*

[b] *École Normale Supérieure de Constantine, Constantine, Algérie*

**e-mail: meryem.aouaouda@gmail.com*

***e-mail: facmath@yahoo.fr*

****e-mail: hisaofujitayashima@qq.com, hisaofujitayashima@yahoo.com*

Received March 15, 2019; revised April 16, 2019; accepted May 15, 2019

Abstract—A mathematical model of the development of a tropical cyclone is considered. It consists of a family of equations obtained by transforming the equation of inviscid non-heat conductive gas (air) motion to the form of equations on wind trajectories in an axially symmetric cylindrical domain. The numerical solution of these equations shows the increase of the wind velocity in accordance with the steam condensation and air warming; later, the velocity becomes stable as the liquid or small pieces of ice accumulate in the air and the friction of water against air decelerates the air updraft.

Keywords: tropical cyclone, wind trajectories, air equations of motion, steam condensation, finite difference method

DOI: 10.1134/S0965542519090045

1. INTRODUCTION

Mathematical modeling of a tropical cyclone has attracted attention of many researchers for a long time, and various models have been proposed (e.g., see [1–9]). Recall that it is known (e.g., see the references mentioned above) that the growth and maintenance of a tropical cyclone mainly depend on the air updraft caused by the latent heat of steam condensation. This mechanism accompanied by the Coriolis force, which causes the circular air motion, and by the friction of water drops (or ice pieces) against air, which decelerates the air updraft.

The aim of this paper is to reveal this mechanism by numerical computations. To this end, using the fundamental equations of fluid dynamics (see [10]) and neglecting viscosity and heat conductivity, we consider the system of equations in an axially symmetric cylindrical domain (see Eqs. (3)–(7)). Since the model under study is reduced to a system of first-order partial differential equations, it is transformed into a family of equations on trajectories (characteristics), which allows us to efficiently compute the desired solution. This idea was partially described in [11].

We solve the equations of the model using a finite difference scheme and partially use the methods developed [12, 13]. However, in these papers the computations were performed only for the vertical air flow. In the present paper, we propose techniques for computing the radial and tangential components of the velocity.

Within the adopted approximation (invariant radius of the cyclone, fixed wind trajectories, zero viscosity and thermal conductivity), the numerical results clearly demonstrate the main features of the tropical cyclone evolution caused by steam condensation, which creates air updraft, and its stabilization due to the friction of water drops against air.

2. MODELING PRINCIPLES AND TRANSFORMATION OF EQUATIONS

Consider the motion of the air inside the tropical cyclone using its approximation in a fixed axially symmetric cylindrical domain. More precisely, consider the motion in the domain

$$\Omega = \{(r, \vartheta, z) \in \mathbb{R}_+ \times [0.2\pi \times \mathbb{R} | (r, z) \in \Gamma_{r,z},\ 0 \le \vartheta < 2\pi\}, \tag{1}$$

$$\Gamma_{r,z} = \{(r,z) \in \mathbb{R}_+ \times \mathbb{R} | 0 < z < \overline{z}_1,\ \Lambda_0(z) < r < \Lambda_1\}. \tag{2}$$

Here, (r, ϑ, z) are the cylindrical coordinates, and the axis z coincides with the axis of the circular air motion. The domain $\{0 < z < \overline{z}_1,\ 0 \le r < \Lambda_0(z)\}$ corresponds to the cyclone eye—the central part of the cyclone with very low pressure. Since the air motion in the eye is different from the motion in the other part of the cyclone, we do not consider it in this paper.

If we assume that all the functions appearing in the equations are independent of ϑ and neglect viscosity and thermal conductivity, then we can write the equations of air motion (see [10]) in the coordinates (r, z) as

$$\frac{\partial \varrho}{\partial t} + \frac{1}{r}\frac{\partial (r\varrho v_r)}{\partial r} + \frac{\partial (\varrho v_z)}{\partial z} = -H_{tr}, \tag{3}$$

$$\varrho\left(\frac{\partial v_r}{\partial t} + v_r\frac{\partial v_r}{\partial r} - \frac{1}{r}v_\vartheta^2 + v_z\frac{\partial v_r}{\partial z}\right) = -R_1\frac{\partial (\varrho T)}{\partial r} + f_0\varrho v_\vartheta - \varepsilon_1(z)v_r, \tag{4}$$

$$\varrho\left(\frac{\partial v_\vartheta}{\partial t} + v_r\frac{\partial v_\vartheta}{\partial r} + \frac{1}{r}v_\vartheta v_r + v_z\frac{\partial v_\vartheta}{\partial z}\right) = -f_0\varrho v_r - \varepsilon_1(z)v_\vartheta, \tag{5}$$

$$\varrho\left(\frac{\partial v_z}{\partial t} + v_r\frac{\partial v_z}{\partial r} + v_z\frac{\partial v_z}{\partial z}\right) = -R_1\frac{\partial (\varrho T)}{\partial z} - [\Sigma + \varrho]g, \tag{6}$$

$$\varrho c_v\left(\frac{\partial T}{\partial t} + v_r\frac{\partial T}{\partial r} + v_z\frac{\partial T}{\partial z}\right) = -R_1\varrho T\left(\frac{\partial v_r}{\partial r} + \frac{1}{r}v_r + \frac{\partial v_z}{\partial z}\right) + L_{tr}H_{tr}. \tag{7}$$

Here, ϱ, T, v_r, v_ϑ, and v_z are, respectively, the density, temperature, radial, tangential, and vertical components of velocity, and the pressure is $R_1\varrho T$ (where R_1 is a constant). In addition, c_v is the specific heat capacity of air, and $f_0 = 2|\omega|\sin\varphi_0$ is the coefficient of the Coriolis force determined by the angular velocity of Earth rotation ω and the latitude of the cyclone center φ_0. In this system of equations, we use for the Coriolis force the approximation that neglects its vertical component and terms related to the vertical component of velocity. On the other hand, the effect of friction between air and the sea surface is represented by the term $-\varepsilon_1(x_3)(v - (v \cdot e_3)e_3)$ in Eqs. (4) and (5), where $\varepsilon_1(x_3)$ is a function that is strictly positive in a neighborhood of $x_3 = 0$ and vanishes for sufficiently large x_3. H_{tr} is the mass of the steam that passes to a liquid or solid phase state in the air updraft, Σ is the amount of liquid or solid phase state in the air, and L_{tr} is the latent heat of H_2O transition from the gaseous state to a liquid or solid state.

Note that, since

$$\frac{1}{r}\frac{\partial (r\varrho v_r)}{\partial r} + \frac{\partial (\varrho v_z)}{\partial z} = \frac{\varrho v_r}{r} + v_r\frac{\partial \varrho}{\partial r} + v_z\frac{\partial \varrho}{\partial z} + \varrho\left(\frac{\partial v_r}{\partial r} + \frac{\partial v_z}{\partial z}\right),$$

we have, in each of Eqs. (3)–(7), the differential transport operator

$$v_r\frac{\partial}{\partial r}\cdot + v_z\frac{\partial}{\partial z}\cdot.$$

This operator determines the wind trajectories on the plane (r, z), which can be calculated. To stress the influence of the processes of condensation, warming, and updraft of the air, which determine the cyclone evolution, we assume that the trajectories on the plane (r, z) thus defined are smooth and relatively stable. By properly selecting the trajectories on the plane (r, z) (this is described in the next section), we transform the system of equations (3)–(7) to a single family of equations on the trajectories.

Assuming that $v_r^2 + v_z^2 > 0$, we set

$$q_r = \frac{v_r}{\sqrt{v_r^2 + v_z^2}}, \quad q_z\frac{v_z}{\sqrt{v_r^2 + v_z^2}}. \tag{8}$$

Define the family of functions $\gamma(s) = (\gamma_r(s), \gamma_z(s))$ determined by the relations

$$\frac{d}{ds}\gamma_r(s) = q_r(\gamma(s)), \quad \frac{d}{ds}\gamma_z(s) = q_z(\gamma(s)). \tag{9}$$

It is clear that, under the assumption of regularity of $(q_r(r,z), q_z(r,z))$, the family of functions γ, which pass through each point (r,z) in $\Gamma_{r,z}$ and satisfy Eqs. (9), fills the domain $\Gamma_{r,z}$.

Assume that the family of functions $\{\gamma\}$ is defined and is independent of t. Then, using the relation

$$v_r\frac{\partial}{\partial r}\varphi(t,r,z)+v_z\frac{\partial}{\partial z}\varphi(t,r,z)=v_\gamma\frac{\partial}{\partial s}\varphi(t,\gamma(s))\equiv v_\gamma\frac{\partial}{\partial s}\varphi(t,s)$$

with $v_\gamma=\sqrt{v_r^2+v_z^2}$, we can write Eqs. (3) and (5) in the form

$$\frac{\partial\varrho}{\partial t}+\frac{\partial(\varrho v_\gamma)}{\partial s}+\frac{\varrho v_r}{r}+\varrho v_\gamma\left(\frac{\partial q_r}{\partial r}+\frac{\partial q_z}{\partial z}\right)=-H_{tr}, \tag{10}$$

$$\frac{\partial v_\vartheta}{\partial t}+v_\gamma\frac{\partial v_\vartheta}{\partial s}+\frac{q_r v_\gamma v_\vartheta}{r}=-f_0 q_r v_\gamma-\frac{\varepsilon_1(z)v_\vartheta}{\varrho}; \tag{11}$$

moreover, using the equality $\varrho\left(\frac{\partial v_r}{\partial r}+\frac{1}{r}v_r+\frac{\partial v_z}{\partial z}\right)=-H_{tr}-\frac{\partial\varrho}{\partial t}-v_\gamma\frac{\partial\varrho}{\partial s}$, which is equivalent to Eq. (3), Eq. (7) can be written as

$$\varrho c_v\left(\frac{\partial T}{\partial t}+v_\gamma\frac{\partial T}{\partial s}\right)-R_1T\left(\frac{\partial\varrho}{\partial t}+v_\gamma\frac{\partial\varrho}{\partial s}\right)=(R_1T+L_{tr})H_{tr}. \tag{12}$$

On the other hand, we multiply Eq. (4) by q_r, Eq. (6) by q_z, and use the equality

$$\frac{\partial q_r^2}{\partial s}+\frac{\partial q_z^2}{\partial s}=0$$

to obtain

$$\varrho\left(\frac{\partial v_\gamma}{\partial s}+v_\gamma\frac{\partial v_\gamma}{\partial s}-\frac{q_r}{r}v_\vartheta^2\right)=-R_1\frac{\partial(\varrho T)}{\partial s}+q_r\varrho f_0 v_\vartheta-[\varepsilon_1(z)q_r^2v_\gamma-q_z g(\varrho+\Sigma)]. \tag{13}$$

To solve this system of equations numerically, we consider the approximate problem obtained by separating the time evolution and spatial structure for v_γ, ϱ, and T (as has been done in [12, 13]). More precisely, put

$$v_\gamma(t,s)=\alpha_\gamma(t)w(t,s) \tag{14}$$

on each trajectory γ (then, $w(t,s)=w(\gamma;t,s)$) and assume that

$$\frac{\partial w}{\partial t}\approx 0,\quad \frac{\partial\varrho}{\partial t}\approx 0,\quad \frac{\partial T}{\partial t}\approx 0. \tag{15}$$

On the other hand, consider $v_\vartheta(t,s)=v_\vartheta(\gamma;t,s)$ for each γ as a function of (t,s); i.e., we do not use the separation of time evolution and spatial structure for $v_\vartheta(t,s)$. Indeed, the evolution of this function is not a direct consequence of the process of steam condensation and air updraft.

To transform Eqs. (10)–(13) to an approximate problem, we use the separation of time evolution and spatial structure introduced in (14)–(15) and define

$$D(t)=D_\gamma(t)=\frac{d}{dt}\alpha_\gamma(t), \tag{16}$$

$$J(s)=J(\gamma;s)=\int_0^s\left(\frac{\partial q_r(r,z)}{\partial r}+\frac{\partial q_z(r,z)}{\partial z}\right)\Bigg|_{(r,z)=\gamma(s')}ds'. \tag{17}$$

Finally, we will use the following expression for H_{tr}:

$$H_{tr}=h_{tr}[v_z]^+=h_{tr}[\alpha(t)q_z w]^+,\quad h_{tr}=\overline{\pi}_{vs}(T)\frac{d}{dz}\log\varrho-\frac{d}{dz}\overline{\pi}_{vs}(T) \tag{18}$$

($[\cdot]^+$ denotes the positive part); this expression was justified, e.g., in [12]. Therefore, assuming that $\varrho > 0$, $w > 0$, $q_z \geq 0$, and replacing $\frac{\partial w}{\partial s}$, $\frac{\partial \varrho}{\partial s}$, and $\frac{\partial T}{\partial s}$ with $\frac{dw}{ds}$, $\frac{d\varrho}{ds}$, and $\frac{dT}{ds}$, we consider on each trajectory γ the following system of equations instead of Eqs. (10)–(13):

$$\frac{d}{ds}(\varrho w) = -q_z w\left(\frac{\overline{\pi}_{vs}(T)}{\varrho}\frac{d\varrho}{dz} - \frac{d\overline{\pi}_{vs}(T)}{dT}\frac{dT}{dz}\right) - \frac{\varrho w}{rJ}\frac{d(rJ)}{ds}, \tag{19}$$

$$\frac{1}{\alpha(t)w}\frac{\partial v_\vartheta}{\partial t} + \frac{\partial v_\vartheta}{\partial s} + \frac{q_r}{r}v_\vartheta = -f_0 q_r - \frac{\varepsilon_1(z)}{\alpha(t)\varrho w}v_\vartheta, \tag{20}$$

$$\varrho c_v \frac{dT}{ds} - R_1 T\frac{d\varrho}{ds} = (R_1 T + L_{tr})q_z\left(\frac{\overline{\pi}_{vs}(T)}{\varrho}\frac{d\varrho}{dz} - \frac{d\overline{\pi}_{vs}(T)}{dT}\frac{dT}{dz}\right), \tag{21}$$

$$\varrho w D(t) + \varrho\left((\alpha(t))^2 w\frac{dw}{ds} - \frac{q_r}{r}v_\vartheta^2\right) = -R_1\frac{d}{ds}(\varrho T) + q_r\varrho f_0 v_\vartheta - [\varepsilon_1(z)\alpha q_r^2 w + q_z g(\varrho + \Sigma)]. \tag{22}$$

Since the trajectories of drops of water or small pieces of ice differ from the air flow trajectories γ, we introduce in Section 4 the amount of liquid or solid water on each air trajectory to be used in practical computations. This will be done after justifying the selection of air trajectories. In Section 4, we also explain the role of the term $D(t)$ in Eq. (22) and set boundary conditions for the air entry and exit in Eqs. (19)–(22).

3. SELECTION OF TRAJECTORIES

We have already seen above that, if we fix the trajectories γ, then the system of equations (3)–(7) for the unknowns ϱ, T, v_r, v_ϑ, and v_z can be reduced to a system of equations for four unknowns ϱ, T, v_γ, and v_ϑ. This allows us to propose an efficient computation technique. However, the trajectories are not actually known. Therefore, for the numerical result to give a valid representation of the processes in the tropical cyclone, the selected trajectories must be good approximations of the actual trajectories. Recall that the literature on the physics of tropical cyclones conventionally assumes that the air moves to the center in the lower part of the cyclone, it moves upwards in the central part, and it moves to the periphery of the cyclone in its upper part. We will also adopt this general scheme of the air flow.

To ensure the validity of the numerical results, the trajectories must be thoroughly selected. In particular, they must be selected such that the family of trajectories does not violate the mass conservation law. That is, if $\overline{\varrho}$ is a t-independent function such that the density ϱ is close to $\overline{\varrho}$ and the trajectories are determined by the velocity field $\overline{v}$ (we will call $\overline{\varrho}$ the basic density and $\overline{v}$ the basic field of velocity), then the quantity $\nabla\cdot(\overline{\varrho v})$ must be sufficiently small. Even if the density ϱ is not known, the basic density $\overline{\varrho}$ can be determined using the hydrostatic principle, and the basic field velocity $\overline{v}$ can be found from the relation $\nabla\cdot(\overline{\varrho v}) \approx 0$, which is in accordance with numerous observations of tropical cyclones.

For the numerical computations, we should select a certain number N of trajectories. We denote them by γ_j, $j = 1,\ldots,N$. According to the assumption made above, each trajectory γ_j consists of three parts: the lower part $\gamma_j^{[1]}$, in which the air moves almost horizontally to the center; the updraft part $\gamma_j^{[2]}$; and the upper part $\gamma_j^{[3]}$, in which the air moves almost horizontally to the periphery. In this paper, we approximate the basic velocity $\overline{v}$ on $\gamma_j^{[1]}$ and $\gamma_j^{[3]}$ by a horizontal flow, so that the behavior of the function w satisfies $rw(r) \approx a_{j,1}$ on $\gamma_j^{[1]}$ and $rw(r) \approx a_{j,3}$ on $\gamma_j^{[3]}$ ($a_{j,1}$ and $a_{j,3}$ are constants). Then, the flows on $\gamma_j^{[1]}$ and $\gamma_j^{[3]}$ are parallel to the axis r on the plane (r,z).

Set

$$\begin{aligned}
\gamma_j &= \gamma_j^{[1]} \cup \gamma_j^{[2]} \cup \gamma_j^{[3]},\\
\gamma_j^{[1]} &= \{(r,z) \in \Gamma_{r,z} \,|\, r_j(z_j^-) \leq r \leq \Lambda_1,\ z = z_j^-\},\\
\gamma_j^{[2]} &= \{(r,z) \in \Gamma_{r,z} \,|\, r = r_j(z),\ z_j^- \leq z \leq z_j^+\},\\
\gamma_1^{[3]} &= \{(r,z) \in \Gamma_{r,z} \,|\, r_j(z_j^+) \leq r \leq \Lambda_1,\ z = z_j^+\}.
\end{aligned} \tag{23}$$

In this structure, the trajectory γ_j forms an angle at the point $(r_j(z_j^-), z_j^-)$ at which $\gamma_j^{[1]}$ joins $\gamma_j^{[2]}$ and at the point $(r_j(z_j^+), z_j^+)$ at which $\gamma_j^{[2]}$ joins $\gamma_j^{[3]}$, and the angles on trajectories do not look natural. However, we believe that these angles do not significantly affect the numerical results.

To select the functions $r_j(z)$ appearing in the definition of $\gamma_j^{[2]}$, we use as the basic density $\overline{\varrho}$ the density distribution of the hydrostatic state of humid air and adopt the empirical value of the ratio between the maximum value of the vertical component $\overline{v}_z$ and the maximum value of the radial component $\overline{v}_r$ of the basic velocity $\overline{v}$. We also assume that $rw(r,z)\big|_{(r,z)\in\gamma_j^{[2]}}$ is not affected by r. This assumption is similar to the assumption adopted for the parts $\gamma_j^{[1]}$ and $\gamma_j^{[3]}$ of the trajectories.

To find the basic density $\overline{\varrho}$, we consider the system of equations for the hydrostatic state of air, which may be humid:

$$\varrho c_v \frac{dT}{dz} - R_1 T \frac{d\varrho}{dz} = \vartheta(z)(R_1 T + L_{tr})(\overline{\pi}_{vs}(T)\frac{d}{dz}\log\varrho - \frac{d}{dz}\overline{\pi}_{vs}(T)), \tag{24}$$

$$R_1 \frac{d}{dz}(\varrho T) = -g\varrho, \tag{25}$$

where $0 \le \vartheta(z) \le 1$ (on the existence and uniqueness of solutions to this system of equations see [13]). The case $\vartheta(z) = 0$ corresponds to the completely dry air, and the case $\vartheta(z) = 1$ corresponds to the saturated humid air. In the latter case, the temperature is distributed such that the condensation process is permanent. As $\overline{\varrho}$, we select the solution to this system of equations with $\vartheta(z) = 1$.

As for the ratio between the maximum value of the vertical component and the maximum value of the radial component of the basic wind velocity, it is different in models of different authors. In this paper, we follow the main trend described in [7] and use

$$\frac{\text{maximum value of } v_z \text{ on } \gamma_j^{[2]}}{\text{maximum value of } |v_r| \text{ on } \gamma_j^{[1]}} \approx \frac{1}{3}. \tag{26}$$

We begin the selection of trajectories by determining the function $\Lambda_0(z)$, which describes the outer boundary of the cyclone eye (see (2)). We set

$$\Lambda_0(z) = \Lambda_0(0)\sqrt{\frac{\overline{\varrho}(0)}{\overline{\varrho}(z)}}. \tag{27}$$

Indeed, in the eye region $\{0 < z < \overline{z}_1, 0 \le r < \Lambda_0(z)\}$ with $\Lambda_0(z)$ defined in (27), if the air moves at the velocity $\overline{v}_0$ with the vertical component independent of z, then we have $\nabla\cdot(\overline{\varrho}\overline{v}_0) = 0$; i.e., the choice of $\Lambda_0(z)$ does not affect the possible motion of air in the eye.

To determine $\gamma_j^{[2]}$ according to the adopted criteria, we assume that

$$rw(r,z)\big|_{(r,z)\in\gamma_j^{[2]}} = a_{j,2}Q, \tag{28}$$

where $a_{j,2}$ is a constant and

$$Q = \frac{1}{\sqrt{9q_z^2 + q_r^2}} = \frac{1}{\sqrt{1 + 8q_z^2}} = \frac{1}{\sqrt{9 - 8q_r^2}}. \tag{29}$$

Since Q is a function depending only on $\frac{q_r}{q_z}$, the quantity $rw(r,z)\big|_{(r,z)\in\gamma_j^{[2]}}$ is determined by the ratio $\frac{q_r}{q_z}$ according to assumption (28). On the other hand, if $(q_r, q_z) = (0,1)$, then $Q = \frac{1}{3}$; and if $(q_r, q_z) = (1,0)$, then $Q = 1$ according to assumption (26).

By assumption (15), we have $\frac{\partial \varrho}{\partial t} \approx 0$, and H_{tr} is relatively small; therefore, by substituting $v_r = \alpha_{\gamma_j} q_r w$ and $v_z = \alpha_{\gamma_j} q_z w$ into (3) and assuming that α_{γ_j} is independent of r and z in the domain represented by the trajectories γ_j, we have

$$\frac{\partial(rw\varrho q_r)}{\partial r} + \frac{\partial(rw\varrho q_z)}{\partial z} \approx 0. \tag{30}$$

Thus, by substituting $rw = a_{j,2}Q$ and $\varrho = \overline{\varrho}(z)$ into (30), we obtain

$$\frac{\partial(Q\overline{\varrho}(z)q_r)}{\partial r} + \frac{\partial(Q\overline{\varrho}(z)q_z)}{\partial z} = 0.$$

Since $\frac{\partial}{\partial r}\overline{\varrho}(z) = 0$, this equality implies

$$-(q_z Q)\frac{d}{dz}\overline{\varrho}(z) = \overline{\varrho}\left(\frac{\partial(Qq_r)}{\partial r} + \frac{\partial(Qq_z)}{\partial z}\right). \tag{31}$$

Rewrite (31) as

$$-(q_z Q)\frac{1}{\varrho}\frac{d}{dz}\overline{\varrho} = q_r\frac{\partial Q}{\partial r} + q_z\frac{\partial Q}{\partial z} + Q\left(\frac{\partial q_r}{\partial r} + \frac{\partial q_z}{\partial z}\right). \tag{32}$$

Expression (29) implies

$$\frac{\partial Q}{\partial r} = \frac{\partial}{\partial r}\frac{1}{\sqrt{9 - 8q_r^2}} = \frac{8q_r}{(9 - 8q_r^2)^{3/2}}\frac{\partial q_r}{\partial r} = 8q_r Q^3\frac{\partial q_r}{\partial r}, \tag{33}$$

$$\frac{\partial Q}{\partial z} = \frac{\partial}{\partial z}\frac{1}{\sqrt{1 + 8q_z^2}} = \frac{-8q_z}{(1 + 8q_z^2)^{3/2}}\frac{\partial q_z}{\partial z} = -8q_z Q^3\frac{\partial q_z}{\partial z}. \tag{34}$$

By substituting (33) and (34) into (32) and using the equalities

$$1 + 8q_r^2Q^2 = \frac{9}{9 - 8q_r^2} = 9Q^2, \quad 1 - 8q_z^2Q^2 = \frac{1}{1 + 8q_z^2} = Q^2,$$

which follow from (29), we finally obtain

$$\frac{\partial q_r}{\partial r} = \frac{1}{9Q^2}\left(-Q^2\frac{\partial q_z}{\partial z} - q_z\frac{1}{\varrho}\frac{d}{dz}\overline{\varrho}\right). \tag{35}$$

Now, we construct $\gamma_j^{[2]}$ ($j = 1,..., N$) by determining r_j one after another (we assume that $r_0(z) = \Lambda_0(z)$). To this end, we use the approximation

$$\frac{d}{dz}(r_j(z) - r_{j-1}(z)) = (r_j(z) - r_{j-1}(z))\frac{1}{q_z}\frac{\partial q_r}{\partial r} + o\left(\left|r_j(z) - r_{j-1}(z)\right|\right). \tag{36}$$

If we replace $\frac{\partial q_r}{\partial r}$ by the expression on the right-hand side of (35) and neglect $o\left(\left|r_j(z) - r_{j-1}(z)\right|\right)$, then we obtain

$$\frac{dr_j(z)}{dz} + \frac{1}{9q_z Q^2}\left(Q^2\frac{\partial q_z}{\partial z} + q_z\frac{1}{\varrho}\frac{d}{dz}\overline{\varrho}\right)r_j(z) = \frac{1}{9q_z Q^2}\left(Q^2\frac{\partial q_z}{\partial z} + q_z\frac{1}{\varrho}\frac{d}{dz}\overline{\varrho}\right)r_{j-1}(z). \tag{37}$$

If we assume that q_z and $\frac{\partial q_z}{\partial z}$ in (37) are equal to their values on $\gamma_{j-1}^{[2]}$, then (37) becomes a linear differential equation for the unknown function $r_j(z)$. By solving Eq. (37), we obtain $r_j(z)$ (and $\gamma_j^{[2]}$) for $j = 1,..., N$ that satisfy the assumptions made above.

4. OTHER CONDITIONS AND DEFINITIONS FOR NUMERICAL SIMULATION

After the trajectories $\gamma_j = \{\gamma_j(s) | 0 \le s \le \overline{s}_j^{-1}\}$ ($j = 1,\ldots,N$) have been selected, we can specify the values of the unknown functions ϱ, v_ϑ, T, and w at the beginning (entry point) of each trajectory γ_j: $\gamma_j(0) = (\Lambda, z_j^-)$. In addition, the unknown $D(t)$ in Eq. (22) allows us to specify a condition at the exit point of each trajectory: $\gamma_j(\overline{s}_j^{-1}) = (\Lambda, z_j^+)$. Thus, we specify four entry conditions

$$\varrho(\gamma_j;t,0) = \overline{\varrho}_j^0, \quad v_\vartheta(\gamma_j;t,0) = \overline{v}_{\vartheta,j}^0, \quad T(\gamma_j;t,0) = \overline{T}_j^0, \quad w(\gamma_j;t,0) = \overline{w}_j^0$$

and one exit condition

$$\varrho(\gamma_j;t,\overline{s}_j^{-1})T(\gamma_j;t,\overline{s}_j^{-1}) = \overline{p}_{*,j}^1.$$

Here $\varrho(\gamma_j;t,s)$ is the density ϱ at the time t at the point $\gamma_j(s)$ ($0 \le s \le \overline{s}_j^{-1}$); and similar notation is used for $T(\gamma_j;t,s)$, $v_\vartheta(\gamma_j;t,s)$, and $w(\gamma_j;t,s)$.

From the viewpoint of the physical model, the conditions at the entry point $\gamma_j(0) = (\Lambda, z_j^-)$ and the exit point $\gamma_j(\overline{s}_j^{-1}) = (\Lambda, z_j^+)$ must coincide with the conditions outside the tropical cyclone; therefore, we assume that the density $\varrho_{ex}(z)$ and temperature $T_{ex}(z)$ outside the cyclone, which are functions of z, are known, and write

$$\overline{\varrho}_j^0 = \varrho_{ex}(z_j^-), \quad \overline{T}_j^0 = T_{ex}(z_j^-), \quad \overline{p}_{*,j}^1 = \varrho_{ex}(z_j^+)T_{ex}(z_j^+).$$

As for $\overline{v}_{\vartheta,j}^0$, in order to make the evolution of v_ϑ independent of the arbitrary choice of the boundary value at the trajectory entry point,we select a small value for $\overline{v}_{\vartheta,j}^0$. On the other hand, since w is the normalized velocity (see (14)), we select for $\overline{w}_j^0$ a constant independent of j. Thus, we have the following conditions:

$$\varrho(\gamma_j;t,0) = \varrho_{ex}(z_j^-), \tag{38}$$

$$w_\vartheta(\gamma_j;t,0) = \overline{v}_\vartheta^0, \tag{39}$$

$$T(\gamma_j;t,0) = T_{ex}(z_j^-), \tag{40}$$

$$w(\gamma_j;t,0) = \overline{w}^0, \tag{41}$$

$$\varrho(\gamma_j;t,\overline{s}_j^{-1})T(\gamma_j;t,\overline{s}_j^{-1}) = \varrho_{ex}(z_j^+)T_{ex}(z_j^+). \tag{42}$$

As for the amount of water in a liquid and solid states Σ in Eq. (22), we note that it is significant only in the part $\gamma_j^{[2]}$, in which the air moves upwards. Therefore, taking into account that the trajectories $\gamma_j^{[2]}$ are inclined and lie one on another, we use the approximation

$$\Sigma_j(t) = \frac{1}{[\tilde{\gamma}_j^+]}\int_0^t \varphi_j(t-s)\int_{[\tilde{\gamma}_j^+]}\left(\overline{\pi}_{vs}(T)\frac{d}{dz}\log\varrho - \frac{d}{dz}\overline{\pi}_{vs}(T)\right)wq_z\,dz\,ds + \beta_j\frac{[\tilde{\gamma}_j^+]}{[\tilde{\gamma}_{j-1}^+]}\Sigma_{j-1}(t), \tag{43}$$

where

$$[\tilde{\gamma}_j^+] = z_j^+ - z_j^- \quad (= \text{altitude of } \gamma_j^{[2]}),$$

$\varphi(\tau)$ is the probability that a drop (or a piece of ice) remains in air after time τ elapsed from the time when this drop (or piece of ice) was created, and β_j is the coefficient representing the amount of liquid or solid water passing from the trajectory γ_{j-1} to the trajectory γ_j.

We solve the system of equations by the finite difference method. Denote by $\{t_k\}$ the discrete time points and by $\{s_{j,i}\}$ the coordinates on the trajectory γ_j, i.e.,

$$0 = t_0 < t_1 < \ldots < t_k < t_{k+1} < \ldots,$$

$$0 = s_{j,0} < s_{j,1} < \ldots < s_{j,i} < s_{j,i+1} < \ldots < s_{j,N_j} = \overline{s}_j^{-1}.$$

Here the coordinates s_j are arranged in the direction of the air flow so that $0 = s_{j,0}$ and $s_{j,N_j} = \overline{s}_j^{-1}$ correspond to the coordinates of the entry and exit points of the air on the trajectory γ_j. We use a uniform time step, $t_{k+1} - t_k = \delta_t$ with a constant δ_t. For the positions $s_{j,i}$, it is convenient to use steps that depend on (j,i), i.e., $s_{j,i+1} - s_{j,i} = \delta_s(j,i)$. This allows us to better describe the structure of trajectories γ_j, while the dependence of the spatial step on (j,i) does not significantly affect the results.

We construct the numerical solution using an explicit finite difference scheme. If we have the solution $(\alpha, \varrho, v_\vartheta, T, w)$ for $t_0, \ldots, t_{k-1}$ on all trajectories, then we can compute $(\alpha, \varrho, v_\vartheta, T, w)$ for t_k as follows.

At the first step, by solving Eq. (20) written in the form

$$\frac{v_\vartheta(t_k, s_{j,i}) - v_\vartheta(t_{k-1}, s_{j,i})}{\delta_t \alpha(t_{k-1}) w(t_{k-1}, s_{i,j})} + \frac{v_\vartheta(t_k, s_{j,i}) - v_\vartheta(t_k, s_{j,i-1})}{\delta_s(j,i)} = F(v_\vartheta, \alpha, \varrho, w)$$

or

$$\begin{aligned}(\delta_s(j,i) + \delta_t \alpha(t_{k-1}) w(t_{k-1}, s_{i,j})) v_\vartheta(t_k, s_{j,i}) &= \delta_s(j,i) v_\vartheta(t_{k-1}, s_{j,i}) \\ + \delta_t \alpha(t_{k-1}) w(t_{k-1}, s_{i,j}) v_\vartheta(t_k, s_{j,i-1}) &+ \delta_s(j,i) \delta_t \alpha(t_{k-1}) w(t_{k-1}, s_{i,j}) F(v_\vartheta, \alpha, \varrho, w),\end{aligned} \tag{44}$$

we find $v_\vartheta(t_k, s_{j,i})$ for $i = 0, \ldots, N_j$ on each trajectory γ_j. Indeed, the condition $v_\vartheta(t_k, s_{j,0}) = \overline{v}_\vartheta^0$ (see (39)) and Eqs. (44) for $i = 1, \ldots, N_j$ determine $v_\vartheta(t_k, s_{j,i})$ for $i = 0, \ldots, N_j$.

Next, we should find $(\varrho(t_k, s_{j,i})$, $T(t_k, s_{j,i})$, and $w(t_k, s_{j,i}))$ for $i = 0, \ldots, N_j$ and $D(t_k) = D_j(t_k)$ on each trajectory γ_j. If α, v_ϑ, and Σ are given and we assign a preliminary value $D^{(m)}$ to $D(t_k) = D_j(t_k)$, then Eqs. (19), (21), and (22) form a system of ordinary differential equations for the unknown functions ϱ, T, and w on each trajectory γ_j. This system subject to initial conditions (38), (40), and (41) can be solved in the conventional way by a finite difference method. Since this solution depends on the preliminary value $D^{(m)}$ specified for $D(t_k) = D_j(t_k)$, the product $\varrho(\gamma_j; t_k, \overline{s}_j^{-1}) T(\gamma_j; t_k, \overline{s}_j^{-1}) = \varrho(t_k, s_{j,N_j}) T(t_k, s_{j,N_j})$, which we denote by $\varrho^{(m)}(t_k, \overline{s}_j^{-1}) T^{(m)}(t_k, \overline{s}_j^{-1})$, also depends on $D^{(m)}$. However, since there is strong correlation between $D^{(m)}$ and $\varrho^{(m)}(t_k, \overline{s}_j^{-1}) T^{(m)}(t_k, \overline{s}_j^{-1})$, which is confirmed by physical considerations and by numerical simulation, we can construct a sequence $\{D^{(m)}\}$ that rapidly converges to $D^{(m_0)}$ such that $\varrho^{(m_0)}(t_k, \overline{s}_j^{-1}) T^{(m_0)}(t_k, \overline{s}_j^{-1})$ satisfies condition (42) with the required accuracy.

At the third (last) step, we find $\alpha(t_k) = \alpha_j(t_k)$ using the simple relation

$$\alpha_j(t_k) = \alpha_j(t_{k-1}) + D_j(t_k) \delta_t. \tag{45}$$

Recall that if we replace $D(t)$ by the derivative $\frac{d}{dt}\alpha(t)$ (see (16)), then (14)–(15) imply that $\varrho w D(t) = \varrho \frac{\partial v_\gamma}{\partial t}$. This allows us to interpret the term $\varrho w D(t)$ in Eq. (22) as the effect due to the equality of the inside and outside pressures at the entry point $\gamma(0)$ and at the exit point $\gamma(\overline{s}_1)$ for the air warmed by the latent steam condensation heat. This effect is similar to the action of the force that pushes the air upward possibly counteracting the friction of the water drops (or ice pieces), which counteracts such an updraft.

5. THE CHOICE OF PHYSICAL PARAMETERS OF THE MODEL

In this section, we give an example of the numerical solution of the proposed model of the tropical cyclone evolution consisting of Eqs. (16), (19)–(22) and conditions (38)–(42). To perform computations according to the known laws of physics, (e.g., see [14, 15]), we must specify the physical parameters

$$g = 9.8 \text{ m/s}^2, \quad R_1 = \frac{R_0}{\mu_a}, \quad c_v = \frac{5}{2}\frac{R}{\mu_a},$$
$$R_0 = 8.314 \text{ J/mol}, \quad \mu_a = 28.96 \text{ g/mol}$$

(here R_0 and μ_a are, respectively, the gas constant and the air molar mass) and define the density function of the saturated steam

$$\overline{\pi}_{vs}(T) = \frac{\mu_h}{R_0 T} E_0 \times 10^{\frac{7.63(T-273.15)}{T-31.25}}, \quad E_0 = 6.107 \text{ mbar}, \quad \mu_h = 18.01 \text{ g/mol} \tag{46}$$

and the latent heat

$$L_{tr}(T) = (3244 - 2.72T) \times 10^3 \text{ (J/kg)}. \tag{47}$$

Since the difference between the densities of the saturated steam near the surface of liquid water and near the ice surface is small and the latent heat of transition of water from the liquid to the solid state is also small, we neglect these differences in our model and use the values specified in (46) and (47), which correspond to the phase transition of H_2O from the gaseous to the liquid state (and conversely).

As the parameter of the Coriolis force, we use the fixed value 3×10^{-5} s^{-1}, which corresponds to its value at the latitude 12° N.

To specify the domain Ω (or $\Gamma_{r,z}$) used in (1) (or (2)), we set $\Lambda_1 = 200$ km and $\overline{z}_1 = 12$ km. We also choose $\Lambda_0(0) = 10$ km, and thus define the function $\Lambda_0(z)$ by formula (27). This corresponds to the model of a tropical cyclone of medium strength.

Here we present the results of computations for eight trajectories γ_j ($j = 1,\ldots,8$). It is clear that such a small number of trajectories is insufficient for detailed computations in the domain $\Gamma_{r,z}$ and construction of the family of trajectories $\{\gamma_j\}$. However, we believe that this number is sufficient for illustrating the behavior of the air flow along these trajectories, and the main stages of the air flow evolution and the entire tropical cyclone can be demonstrated.

For selecting the trajectories γ_j ($j = 1,\ldots,8$), we assume that the humidity of the air entering the cyclone domain Ω is 50%, and the air humidity at the exit of Ω is 100%. Then, we find the distribution of density $\tilde{\varrho}_1(z)$ by solving Eqs. (24), (25) with

$$\vartheta(z) = \begin{cases} 1/2 & \text{for} \quad 0 \le z \le \overline{\zeta}_M, \\ 1 & \text{for} \quad \overline{\zeta}_M < z \le \overline{z}_1, \end{cases} \tag{48}$$

where $\overline{\zeta}_M$ is chosen such that $\{r = \Lambda_1,\ 0 < z < \overline{\zeta}_M\}$ is the inflow boundary ($v_r < 0$) and $\{r = \Lambda_1,\ \overline{\zeta}_M < z < \overline{z}_1\}$ is the outflow boundary ($v_r > 0$). The formal computation of $\overline{\zeta}_M$ is not so straightforward, but its numerical approximation can be constructed. Using this function $\tilde{\varrho}_1(z)$, we set

$$M_\varrho = \int_0^{\overline{z}_1} \tilde{\varrho}_1(z)dz, \tag{49}$$

and determine z_j^- and z_j^+ (see (23)) using the relations

$$\int_0^{z_j^-} \tilde{\varrho}_1(z')dz' = \frac{4j-2}{61} M_\varrho, \quad j = 1,\ldots,8, \tag{50}$$

$$\int_0^{z_j^+} \tilde{\varrho}_1(z')dz' = \frac{4(16-j)+2}{61} M_\varrho, \quad j = 3,\ldots,8, \tag{51}$$

$$\int_0^{z_2^+} \tilde{\varrho}_1(z')dz' = \frac{57.5}{61} M_\varrho, \tag{52}$$

$$\int_0^{z_1^+} \tilde{\varrho}_1(z')dz' = \frac{60}{61} M_\varrho. \tag{53}$$

The values of z_j^- and z_j^+ thus found are shown in Table 1.

Table 1

γ_j	z_j^- (km)	z_j^+ (km)
γ_1	$z_1^- = 0.23$	$z_1^+ = 11.71$
γ_2	$z_2^- = 0.70$	$z_2^+ = 10.77$
γ_3	$z_3^- = 1.20$	$z_3^+ = 9.01$
γ_4	$z_4^- = 1.72$	$z_4^+ = 7.91$
γ_5	$z_5^- = 2.28$	$z_5^+ = 6.94$
γ_6	$z_6^- = 2.86$	$z_6^+ = 6.05$
γ_7	$z_7^- = 3.48$	$z_7^+ = 5.25$
γ_8	$z_8^- = 4.25$	$z_8^+ = 4.50$

The trajectories constructed using Eq. (36) with these z_j^- and z_j^+ are shown in Fig. 1.

Under conditions (38), (40), and (42), we use the density $\varrho_{ex}(z)$ and temperature $T_{ex}(z)$ outside the cyclone zone. As the functions $\varrho_{ex}(z)$ and $T_{ex}(z)$, we use the solution to the system of equations (24), (25) with

$$\vartheta(z) = \begin{cases} 1/3 & \text{for} \quad 0 \le z \le \overline{\zeta}_M, \\ 2/3 & \text{for} \quad \overline{\zeta}_M < z \le \overline{z}_1. \end{cases} \tag{54}$$

Note that condition (48) corresponds to an intermediate humidity between condition (54) and the total humidity $\vartheta(z) \equiv 1$ corresponding to $\overline{\varrho}$.

As the function $\varphi_j(\tau)$ in expression for Σ_j (see (43)), we use the function

$$\varphi_j(\tau) = \exp\left(\frac{\pi\tau^2}{4b_j^2}\right) \tag{55}$$

with

$$b_j = \begin{cases} 600 \text{ s } (= 10 \text{ min}) & \text{for} \quad \gamma_j, \quad j = 1,2,3,4,5, \\ 480 \text{ s } (= 8 \text{ min}) & \text{for} \quad \gamma_6, \\ 300 \text{ s } (= 5 \text{ min}) & \text{for} \quad \gamma_7, \\ 120 \text{ s } (= 2 \text{ min}) & \text{for} \quad \gamma_8. \end{cases} \tag{56}$$

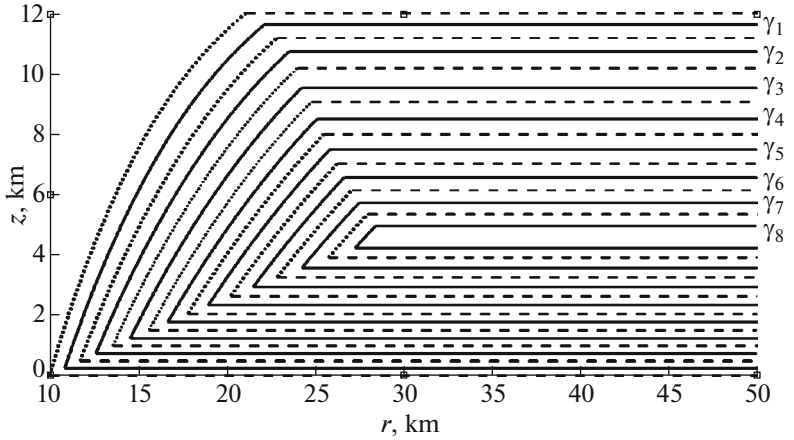

Fig. 1. The family of trajectories on the plane (r, z) (up to 50 km from the center).

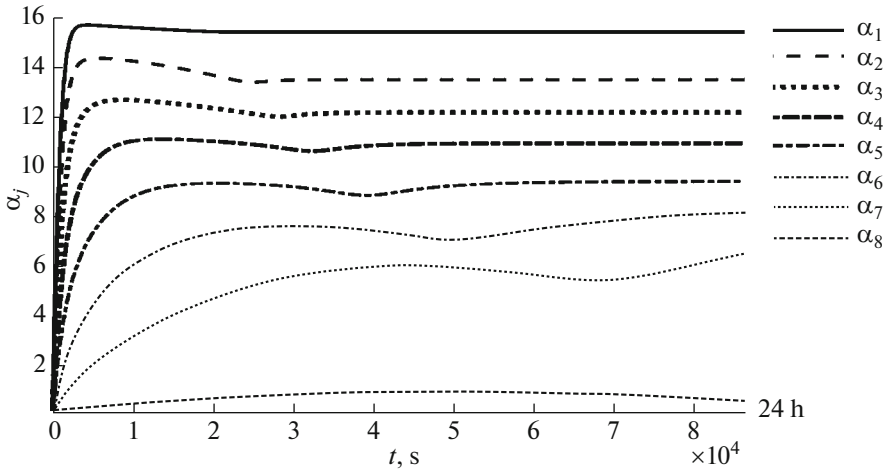

Fig. 2. Evolution of the intensity coefficients $\alpha_j(t)$ during 24 h.

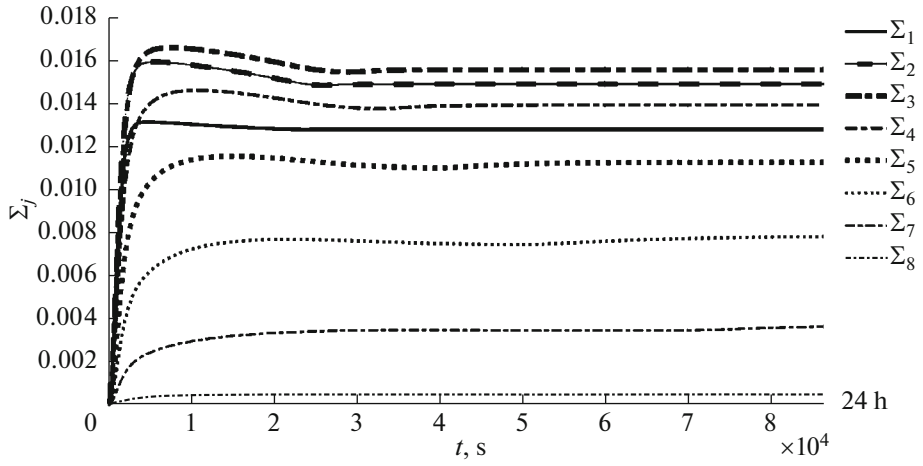

Fig. 3. Evolution of the amount of the liquid or solid water $\Sigma_j(t)$ during 24 h.

Recall that

$$\int_0^\infty \varphi_j(\tau)dr = b_j,$$

i.e., b_j is the mean time during which a drop (little piece of ice) remains in air after its formation. On the other hand, for the coefficients β_j, which are also used in the expression for Σ_j (see (43)), use the condition

$$\beta_j = \begin{cases} \frac{1}{2} & \text{for} \quad \gamma_j, \quad j = 2,3,4, \\ \frac{2}{3} & \text{for} \quad \gamma_j, \quad j = 5,6,7, \\ \frac{1}{3} & \text{for} \quad \gamma_8. \end{cases} \tag{57}$$

For the function $\varepsilon_1(z)$, which represents the effect of friction between the air and the sea surface, we set

$$\varepsilon_1(z) = \begin{cases} 8\times 10^{-5} & \text{on } \gamma_1, \\ 0 \quad \text{on} & \gamma_j, \quad j = 2,\ldots,8. \end{cases} \tag{58}$$

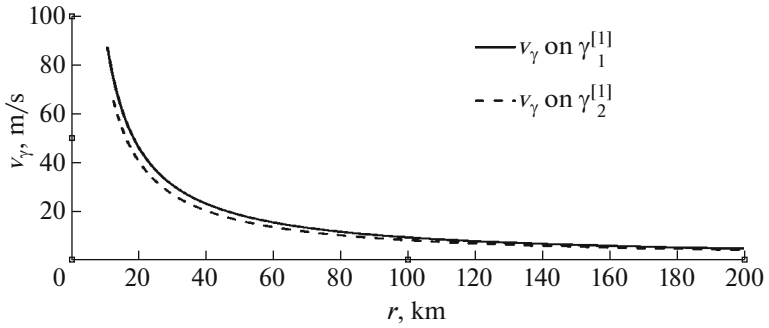

Fig. 4. The component v_γ of the wind velocity in the direction of γ in the lower part of γ_1 and γ_2 after 24 h.

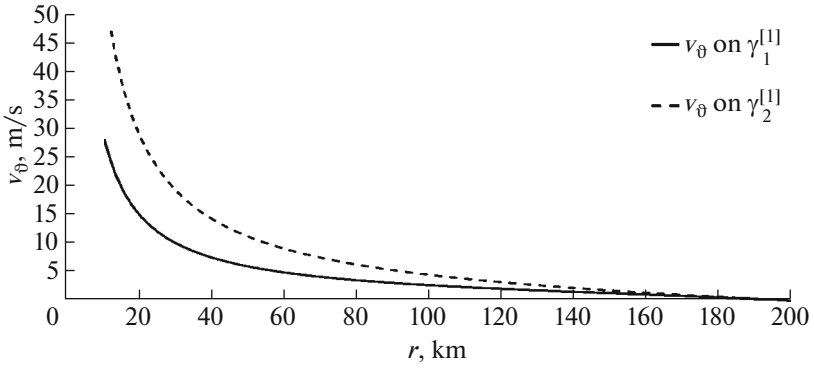

Fig. 5. The tangential component v_ϑ of the wind velocity in the lower part of γ_1 and γ_2 after 24 h.

6. NUMERICAL RESULTS

In this section, we describe the numerical results obtained during simulation. Figure 2 illustrates the evolution of the intensity coefficients $\alpha_j(t)$ on the trajectories γ_j ($j = 1,\ldots,8$). The computations were performed with the time step 50 s.

The evolution of air flow velocity on the trajectories γ_j is accompanied by the increase of the mass of water in the liquid or solid state $\Sigma_j(t)$ as shown in Fig. 3. It is seen that there is strong correlation between $\alpha_j(t)$ and $\Sigma_j(t)$.

In addition, note that in the proposed model the cyclone evolves fairly quickly: it achieves its mature structure in less than 24 hours. Figure 4 shows the profile of the component v_γ of the wind velocity in the direction of trajectories, and Fig. 5 shows the profile of the tangential component v_ϑ of the wind velocity in the lower part of the trajectories γ_1 and γ_2 after 24 hours. The velocity is measured in m/s. Note that the tangential velocity on γ_2 is greater than on γ_1.

This suggests that the friction against the ocean surface, which decelerates the air flow near the ocean–atmosphere boundary, has a significant effect. Figure 6 shows that the tangential component of the wind velocity in the upper part of γ_2 has the same direction as in its lower part, and the tangential component on γ_1 in the peripheral part of the cyclone has the opposite direction. We believe that this difference is explained by the fact that the influence of friction against the sea surface on the trajectory γ_2 is very small; therefore, the Coriolis force has the same effect in the lower part as in the upper part of the trajectory. On the other hand, the friction against the sea surface in the lower part of γ_1 also slows down v_ϑ, while there is no friction in the upper part; for this reason, in the upper part of γ_1, v_ϑ is pushed in the opposite direction by the Coriolis force. The fact that the friction effect is less pronounced in the numerical result for the component in the direction of trajectory can be explained as a consequence of using fixed trajectories for the simulation.

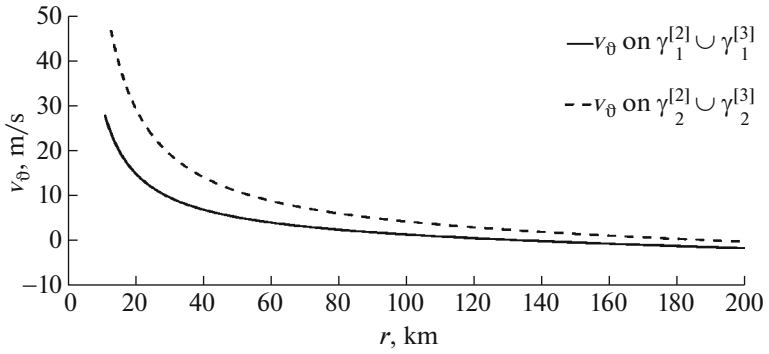

Fig. 6. The tangential component v_ϑ of the wind velocity in the upper part γ_1 and γ_2 after 24 h.

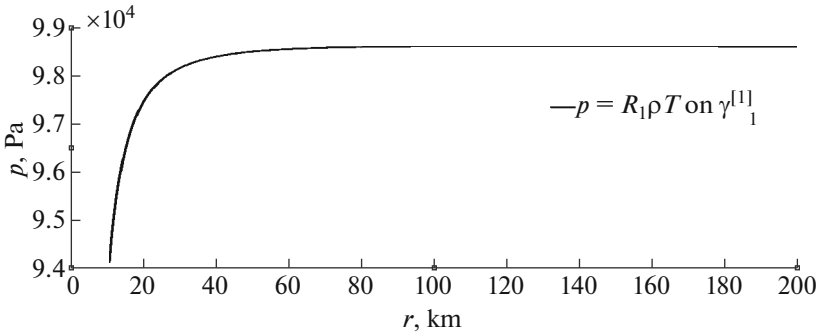

Fig. 7. The pressure $p = R_1 \varrho T$ in the lower part of γ_1 after 24 h.

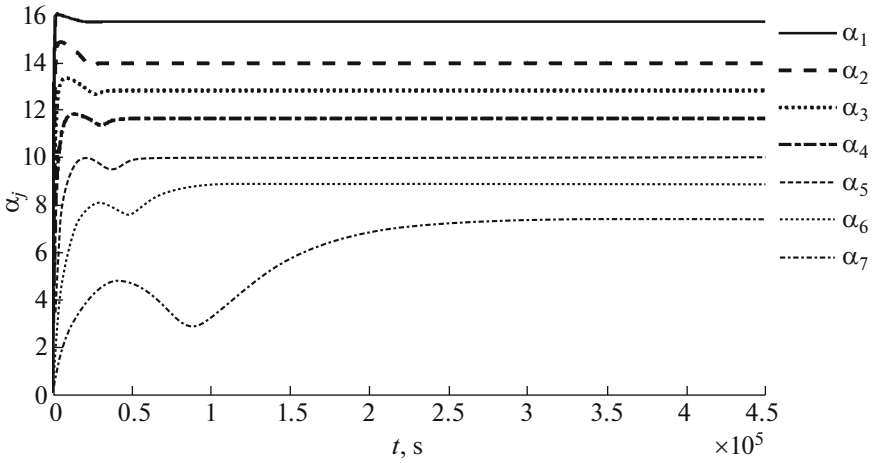

Fig. 8. Evolution of the intensity coefficients $\alpha_j(t)$ during five days.

The profile of the pressure $p = R_1 \varrho T$ in the lower part of γ_1 (230 m above the sea level) after 24 hours is shown in Fig. 7.

Figures 4–7 show that the model proposed in this paper gives a reasonably good description of the structure of the tropical cyclone.

Let us also illustrate the evolution of the intensity coefficients $\alpha_j(t)$ and of the amount of water in the liquid or solid state $\Sigma_j(t)$ during five days. It is seen in Figs. 8 and 9, that $\alpha_j(t)$ and $\Sigma_j(t)$ become approx-

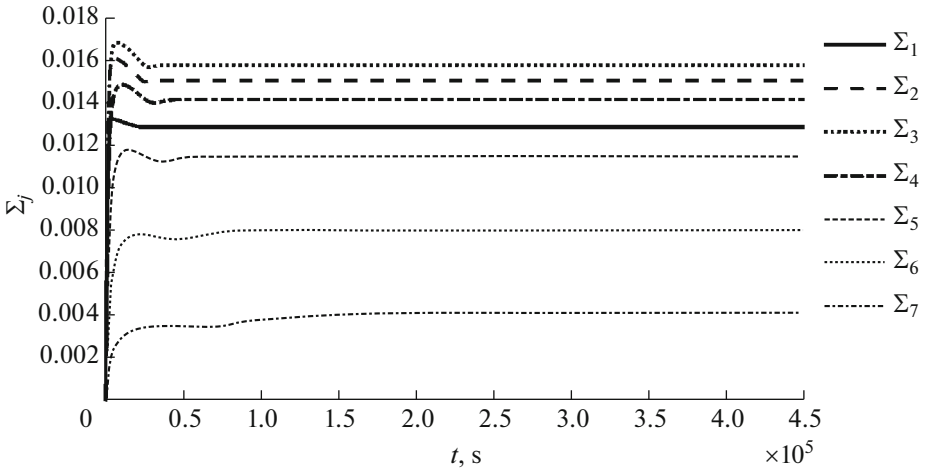

Fig. 9. Evolution of the amount of the liquid or solid water $\Sigma_j(t)$ during five days.

imately stable. However, we also note that the stabilization is fast on the trajectories on which the amount of liquid or solid water is large, while the stabilization is slow on the trajectories on which $\Sigma_j(t)$ is small. We did not show the evolution of $\alpha_8(t)$ and $\Sigma_8(t)$ in Figs. 8 and 9 on the trajectory γ_8 because the numerical solution $\alpha_8(t)$ and $\Sigma_8(t)$ becomes negative at certain points in time, which has no physical meaning.

The proposed model of the tropical cyclone also has a steady-state solution. The values of the intensity coefficients α_j and the amount of liquid or solid water Σ_j in the steady-state solution are shown in Table 2. It is seen that when Σ_j is large, $\alpha_j(t)$ and $\Sigma_j(t)$ rapidly converge to the corresponding values of the of steady-state solution. Also note that the amount of liquid or solid water on γ_8 is very low compared with the other values of Σ_j for $j = 1,\ldots,7$. In our opinion, this is the cause of the relative instability of the solution on γ_8.

7. CONCLUSIONS AND PROSPECTS

A system of equations for describing the motion of air along a family of trajectories under the assumption of axial symmetry was proposed. The numerical results reveal the main aspects of the air motion evolution caused by moisture condensation with account for the latent heat of steam generation and friction of water drops and little pieces of ice against air, which slows down the updraft. The distribution of wind velocity and pressure after 24 hours after the initial time obtained by the numerical computations coincides with the overall characteristics of a tropical cyclone of medium strength. We interpret the obtained rate of the cyclone evolution, which significantly exceeds the observation data, as a consequence of the difference between the model problem statement from reality, in which other factors, in addition to the basic cyclone development mechanism, are involved.

Table 2

γ_j	α_j	Σ_j
γ_1	15.3434	0.0131
γ_2	13.4317	0.0153
γ_3	12.1234	0.0160
γ_4	10.8862	0.0143
γ_5	9.3652	0.0115
γ_6	8.0594	0.0080
γ_7	6.2224	0.0037
γ_8	0.4936	0.000457

The proposed model is based on the description of fixed trajectories (on the plane (r, z)), which facilitates the numerical solution. However, it is clear that these trajectories must be determined by the self-consistent air motion. In particular, the following important factors must be taken into account for the cyclone description.

1. The effect of growth of the velocity tangential component, which creates the centrifugal force and thus pushes the air upwards in the lower part of the trajectories.

2. Expansion of the cyclone zone in the process of evolution.

3. The effect of turbulent air motion.

In our future research, we are going to improve the model by taking into account these factors. The displacement of the cyclone as a whole should also be taken into account. However, the simulation of this phenomenon in the statement proposed in this paper requires the development of new techniques.

ACKNOWLEDGMENTS

We are grateful to Prof. O. Díaz Rodríguez from the Institute of Meteorology, Habana (Cuba) for elucidating the physical aspects of tropical cyclones and to Dr. D. Remaoun Bourega from the Science and Technology University, Oran (Algerie) for help in numerical computations. We are also grateful to S.L. Skorokhodov from the Dorodnicyn Computing Center, Federal Research Center "Computer Science and Control," Russian Academy of Sciences, Moscow for his help in preparing the text of the paper.

REFERENCES

1. A. P. Khain, *Mathematical Modeling of Tropical Cyclones*(Gidrometeoizdat, Leningrad, 1984) [in Russian].
2. W. Cotton, G. Bryan, and S. van den Heever, *Storm and Cloud Dynamics,* 2nd ed. (Academic Press, 2011).
3. V. Ooyama Katsuyuki, "Conceptual evolution of the tropical cyclone," J. Meteor. Soc. Japan. **60**, 369–379 (1981).
4. K. A. Emanuel, "An air-sea interaction theory for tropical cyclones. Part I: Steady-state maintenance," J. Atmos. Sci. **43**, 585–604 (1986).
5. R. Rotunno and K. A. Emanuel, "An air-sea interaction theory for tropical cyclones. Part II: Evolutionary study using a non-hydrostatic axisymmetric numerical model," J. Atmos. Sci. **44**, 542–561 (1987).
6. G. J. Holland, "The maximum potential intensity of tropical cyclones," J. Atmos. Sci. **54**, 2519–2541 (1997).
7. J. P. Camp and M. T. Montgomery, "Hurricane maximum intensity: Past and present," Monthly Weather Rev. **129**, 1704–1717 (2001).
8. V. I. Vlasov, S. L. Skorokhodov, and H. Fujita Yashima, "Simulation of air flow in a typhoon lower layer," Russ. J. Num. Anal. Math. Mod. **26**, 85–111 (2011).
9. M. T. Montgomery and R. K. Smith, "Recent developments in the fluid dynamics of tropical cyclones," Trop. Cycl. Res. Rep. **1**, 1–24 (2016).
10. L. D. Landau and E. M. Lifshitz, *Fluid Mechanics,* 2nd ed. (Nauka, Moscow, 1986; Pergamon Press, Oxford, 1987).
11. H. Fujita Yashima, "Simulation of the internal structure of tropical cyclones: The flow equation on wind trajectories," Itogi Nauki Tekh., Ser.: Sovr. Mat. Pril. **137**, 118–130 (2017).
12. S. Ghomrani, J. Marín Antuña J., and H. Fujita Yashima, "Un modelo de la subida del aire ocasionada por la condensación del vapor y su cálculo numeric," Rev. Cuba Fís. **32**, 3–8 (2015).
13. D. Remaoun Bourega, M. Aouaouda, and H. Fujita Yashima, "Oscillation de la pluie dans un modèle mathématique de l'orage," Ann. Math. Afr. **7**, 19–35 (2018).
14. A. K. Kikoin and I. K. Kikoin, *Molecular Physics* (Nauka, Moscow, 1976) [in Russian].
15. L. T. Matveev, *Foundations of General Meteorology: Physics of the Atmosphere* (Gidrometeoizdat, St. Petersburg, 2000) [in Russian].

Translated by A. Klimontovich